

Global sensitivity analysis of the Rodgers and Rowland model for prediction of tissue: plasma partitioning coefficients: Assessment of the key physiological and physicochemical factors that determine small-molecule tissue distribution

Estelle Yau^{1,2}, Andrés Olivares-Morales^{2,*}, Michael Gertz², Neil Parrott², Adam S. Darwich^{1,3}, Leon Aarons² and Kayode Ogungbenro²

¹ Centre for Applied Pharmacokinetic Research (CAPKR), The University of Manchester, Manchester, UK

² Roche Pharma and Early Development, Pharmaceutical Sciences, Roche Innovation Center Basel, Switzerland

³ Current affiliation: Logistics and Informatics in Health Care, School of Engineering Sciences in Chemistry, Biotechnology and Health (CBH), KTH Royal Institute of Technology, Stockholm, Sweden

*To whom correspondence should be addressed.

*Corresponding author:

Andrés Olivares-Morales

Roche Pharma and Early Development (pRED), Roche Innovation Center Basel, F. Hoffmann-La Roche Ltd,
Grenzacherstrasse 124, 4070 Basel, Switzerland

Email address: andres.olivares@roche.com

Running title (max 50 characters, including spaces): Sensitivity analysis of model for Kpu prediction

Keywords (5 max): Global sensitivity analysis, drug distribution, PBPK, partition coefficients, uncertainty

1
2 **Global sensitivity analysis of the Rodgers and Rowland model for prediction of tissue: plasma partitioning**
3 **coefficients: Assessment of the key physiological and physicochemical factors that determine small-molecule**
4 **tissue distribution**

5
6 Estelle Yau^{1,2}, Andrés Olivares-Morales^{2,*}, Michael Gertz², Neil Parrott², Adam S. Darwich^{1,3}, Leon Aarons² and
7 Kayode Ogungbenro²

8
9 ¹ Centre for Applied Pharmacokinetic Research (CAPKR), The University of Manchester, Manchester, UK
10 ² Roche Pharma and Early Development, Pharmaceutical Sciences, Roche Innovation Center Basel, Switzerland
11 ³ Current affiliation: Logistics and Informatics in Health Care, School of Engineering Sciences in Chemistry,
12 Biotechnology and Health (CBH), KTH Royal Institute of Technology, Stockholm, Sweden

13 *To whom correspondence should be addressed.

14

15 *Corresponding author:
16 Andrés Olivares-Morales
17 Roche Pharma and Early Development (pRED), Roche Innovation Center Basel, F. Hoffmann-La Roche Ltd,
18 Grenzacherstrasse 124, 4070 Basel, Switzerland
19 Email address: andres.olivares@roche.com

20

21 **Running title** (max 50 characters, including spaces): Sensitivity analysis of model for Kpu prediction

22

23 **Keywords** (5 max): Global sensitivity analysis, drug distribution, PBPK, partition coefficients, uncertainty

24

25 (Word count: 6271; 3 tables, 4 figures)

26

27 **Abstract**

28 In physiologically-based pharmacokinetic (PBPK) modelling, the large number of input parameters,
29 limited amount of available data and the structural model complexity generally hinder simultaneous estimation
30 of uncertain and/or unknown parameters. These parameters are generally subject to estimation. However, the
31 approaches taken for parameter estimation vary widely. Global sensitivity analyses are proposed as a method to
32 systematically determine the most influential parameters that can be subject to estimation. Herein, a global
33 sensitivity analysis was conducted to identify the key drug and physiological parameters influencing drug
34 disposition in PBPK models and to potentially reduce the PBPK model dimensionality. The impact of these
35 parameters was evaluated on the tissue-to-unbound plasma partition coefficients (K_{pu}) predicted by the
36 Rodgers and Rowland model using Latin hypercube sampling combined to partial rank correlation coefficients
37 (PRCC). For most drug classes, PRCC showed that LogP and fraction unbound in plasma (f_{u_p}) were generally the
38 most influential parameters for K_{pu} predictions. For strong bases, blood:plasma partitioning was one of the most
39 influential parameter. Uncertainty in tissue composition parameters had a large impact on K_{pu} and V_{ss}
40 predictions for all classes. Amongst tissue composition parameters, changes in K_{pu} outputs were especially
41 attributed to changes in tissue acidic phospholipid concentrations and extracellular protein tissue:plasma ratio
42 values. In conclusion, this work demonstrates that for parameter estimation involving PBPK models and
43 dimensionality reduction purposes, less influential parameters might be assigned fixed values depending on the
44 parameter space, while influential parameters could be subject to parameters estimation.

45

46 Word count: 242

47 **Introduction**

48 Physiologically-based pharmacokinetic (PBPK) models are complex mechanistic models which are used
49 during all stages of drug development for various analyses (e.g., *in vitro-in vivo* extrapolation (IVIVE), interspecies
50 extrapolation and predictions of drug exposure (1-3)). Key parameters in PBPK models are tissue:unbound
51 plasma partition coefficients (K_{pu}). They describe the extent of drug distribution in each organ/tissue and are
52 defined as the ratio of the tissue drug concentration to the unbound plasma concentration at steady state. In
53 drug discovery and early development stages, K_{pu} can also be used to predict the volume of distribution at
54 steady state (V_{ss}), a key pharmacokinetic parameter describing the overall drug distribution within the body
55 relevant for selecting the first dose in human and dosing frequency. As *in vivo* K_{pu} measurements require
56 excessive resources in terms of animals numbers and bioanalytics for the large number of compounds considered
57 during drug discovery, these experiments are not usually performed at this stage. Instead, several approaches
58 have been proposed to predict K_{pu} from *in vitro* and *in silico* data (4-7).

59 The models proposed by Rodgers and Rowland (5, 8, 9) are one of the most commonly used method. In an
60 analysis comparing models to predict tissue:plasma partition coefficients (K_p), Graham *et al.* reported that the
61 Rodgers and Rowland (R&R) model was the most accurate for rat K_p predictions with 77% within three-fold of
62 experimental values and the second most accurate for rat V_{ss} prediction with 80% within three-fold (10).
63 Similarly, for human V_{ss} , the PhRMA consortium reported that the R&R model had the best prediction accuracy
64 with 78% of compounds within three-fold compared to five other mechanistic methods (11). The main
65 assumptions of the R&R model are that drugs partition into neutral lipids and neutral phospholipids of tissue
66 cells, and also partition within intra- and extra- cellular tissue water. Additionally, the electrostatic interactions
67 that form between basic drugs and tissue acidic phospholipids (AP) are incorporated for compounds with $pK_a \geq 7$,
68 while acids interact with extracellular proteins (PR) and weakly basic compounds bind predominately to albumin
69 and neutral drugs to lipoproteins (5, 8). The R&R model has many input parameters: drug specific input
70 parameters are experimentally measured or calculated *in silico* from empirical models; and tissue composition
71 parameters are set values reported in the literature for an individual or average subject of the target species.
72 And although sometimes overlooked, variability and uncertainty do exist regarding the true value of each input
73 parameter for a particular chemical/bioanalytical assay or a particular group of animals or human population:
74 uncertainty in the measured values, lack of information, inter/within species variability, etc.

75 During PBPK model development, the K_{pu} s predicted by the R&R model, or similar models, are usually
76 considered as point estimates to simulate drug distribution into tissues. Simulations are then typically validated
77 against observed *in vivo* plasma pharmacokinetic data from pre-clinical species (namely mice, rat, dog and non-
78 human primates) and humans. If a mismatch exists additional studies may be performed to enable a mechanistic
79 understanding of the reasons for the difference. However, if differences cannot be explained then it is common

80 practice to adjust parameter estimates to fit the experimental data. The complexity of the PBPK model structure,
81 the large number of input parameters and the limited data available generally hinder estimation of uncertain or
82 unknown model parameters. Heterogeneous and subjective approaches for parameter estimation using PBPK
83 models exist in the literature (12-17). For instance, modellers generally fit a few specific K_{pus} as pharmacokinetic
84 data become available while fixing others subjectively. This may lead to inaccurate parameter estimates or
85 underestimation of uncertainty, and overall poor extrapolation. Bayesian methods could be a powerful approach
86 for aiding parameter estimation of PBPK models (18). The current work is a first step to reduce PBPK model
87 dimensionality by assessing the sensitivities and excluding non-influential parameters (K_{pus}) and model states
88 (tissue compartments) as recommended by recent regulatory guidelines (19, 20). The comprehensive sensitivity
89 analysis (SA) was also conducted to identify key parameters responsible for variability/uncertainty in predicted
90 drug distribution (K_{pus} and V_{ss}).

91 **Methods**92 **Rodgers and Rowland model**

93 The current work is focussed exclusively on the R&R equations as previous work had shown that it gave the
 94 highest degree of prediction accuracy for Kpu values (21). More details of these equations can be found in the
 95 original articles (5, 8, 9). The R&R model includes one equation for the prediction of Kpu for moderate-to-strong
 96 bases with one $pK_a \geq 7$ (Eq. 1) and a second equation for other drug classes (Eq. 2):

$$Kpu = \left(\frac{X \cdot f_{IW}}{Y} \right) + f_{EW} + \left(\frac{P \cdot f_{NL} + (0.3P + 0.7) \cdot f_{NP}}{Y} \right) + \left(\frac{Ka_{AP} \cdot [AP^-]_T \cdot (X - 1)}{Y} \right) \quad (1)$$

$$Kpu = \left(\frac{X \cdot f_{IW}}{Y} \right) + f_{EW} + \left(\frac{P \cdot f_{NL} + (0.3P + 0.7) \cdot f_{NP}}{Y} \right) + (Ka_{PR} \cdot [PR]_T) \quad (2)$$

97 where P is the octanol:water partition coefficient for all tissues except adipose (vegetable oil:water). The
 98 vegetable oil:water partition coefficient, $\text{LogP}_{vo:w}$, is calculated as : $\text{LogP}_{vo:w} = 1.115 \cdot \log P_{o:w} - 1.35$.
 99 f is the fractional tissue volume and subscripts EW and IW refer to extra- and intra-cellular tissue water, NL and
 100 NP refer to neutral lipids and neutral phospholipids, respectively ; $[AP^-]_T$ and $[PR]_T$ are the tissue concentrations
 101 of acidic phospholipids (AP) and extracellular albumin (for acids and weak bases) or lipoprotein (for neutrals),
 102 respectively; Ka_{AP} and Ka_{PR} are the association constants of the drug compound with AP and either extracellular
 103 albumin or lipoprotein, respectively; and X and Y are terms accounting for the drug ionisation in intracellular
 104 water and in plasma defined as follows:

105 For monoprotic bases: $= 1 + 10^{pK_a - pH_{IW}}$, $Y = 1 + 10^{pK_a - pH_p}$

106 For monoprotic acids: $= 1 + 10^{pH_{IW} - pK_a}$, $Y = 1 + 10^{pH_p - pK_a}$

107 For neutrals: $X = Y = 1$ (*no ionisation*). pH_{IW} : pH of the intracellular water (7), pH_p : pH of plasma (7.4) (5)

108

109 Ka_{AP} represents an overall affinity constant for various AP. The model makes the assumption that Ka_{AP} in
 110 red blood cells (RBCs) is representative of the Ka_{AP} in all tissues. Furthermore, the model assumes that Ka_{PR}
 111 determined from the plasma data is representative of the Ka_{PR} in all tissues; where Ka_{PR} represents the affinity
 112 constant to extracellular binding proteins. The affinity constants to bind to Ka_{AP} and Ka_{PR} were determined from
 113 Kpu_{RBC} or f_{u_p} data/information using equations 3 and 4, respectively.

$$Ka_{AP} = \left[Kpu_{RBC} - \left(\frac{1 + 10^{pK_a - pH_{RBC}}}{Y} \cdot f_{IW,RBC} \right) - \left(\frac{P \cdot f_{NL,RBC} + (0.3P + 0.7) \cdot f_{NP,RBC}}{Y} \right) \right] \cdot \left(\frac{Y}{[AP^-]_{RBC} \cdot 10^{pK_a - pH_{RBC}}} \right) \quad (3)$$

$$Ka_{PR} = \left[\frac{1}{f_{u_p}} - 1 - \left(\frac{P \cdot f_{NL_p} + (0.3P + 0.7) \cdot f_{NP_p}}{Y} \right) \right] \cdot \frac{1}{[PR]_p} \quad (4)$$

114 where subscripts RBC and P indicate red blood cells and plasma, respectively; pH_{RBC} is the intracellular pH of red
115 blood cells (7.22) (5); fu_p is the unbound fraction of drug in plasma; and Kpu_{RBC} is the red blood cell:plasma water
116 concentration ratio.

117 Kpu_{RBC} can be determined *in vitro* or calculated from fu_p , blood:plasma ratio (BP) and the haematocrit using
118 equation 5 (22, 23):

$$Kpu_{RBC} = \frac{Haematocrit - 1 + BP}{fu_p \cdot Haematocrit} \quad (5)$$

119 Using these equations, negative values can be obtained for Ka_{AP} and Ka_{PR} , in such a case the affinity constants
120 are set to zero (9).

121

122 By decomposing the R&R model (Eq. 1 and 2), three terms can actually be distinguished and each can dominate
123 the Kpu outputs under certain circumstances:

124 - Term 1 ($\left(\frac{X \cdot f_{IW}}{Y}\right) + f_{EW}$), related to fractional tissue water volumes (f_{IW} , f_{EW}) and is only pKa-dependent: it has
125 the greatest relevance if terms 2 and 3 are negligible (e.g., high fu_p - low LogP compound). Under such
126 conditions, the distribution space is the total water.

127 - Term 2 ($\frac{P \cdot f_{NL} + (0.3P + 0.7) \cdot f_{NP}}{Y}$), related to tissue lipid partitioning (neutral lipids (f_{NL}), and neutral phospholipids
128 (f_{NP})) and is LogP- and pKa-dependent: it might be the most relevant term when Ka_{AP} or Ka_{PR} are zero.

129 - Term 3 ($\frac{Ka_{AP} \cdot [AP^-]_T \cdot (X-1)}{Y}$ or $Ka_{PR} \cdot [PR]_T$), related to interactions with tissue AP ($Ka_{AP} \cdot [AP^-]_T$) or nonspecific
130 protein binding ($Ka_{PR} \cdot [PR]_T$), is dependent on LogP, pKa, fu_p (and BP for strong bases). It has relevance if
131 partitioning into RBCs lipids or into plasma lipids is greater than binding to RBCs or to plasma proteins (e.g.,
132 low fu_p relative to LogP), i.e. : $\left(\frac{1+10^{pKa-pH_{RBC}}}{Y} \cdot f_{IW,RBC}\right) + \left(\frac{P \cdot f_{NL,RBC} + (0.3P + 0.7) \cdot f_{NP,RBC}}{Y}\right) \geq \frac{Haematocrit - 1 + BP}{fu_p \cdot Haematocrit}$

133 from equations 3 and 5, or $1 + \left(\frac{P \cdot f_{NL,p} + (0.3P + 0.7) \cdot f_{NP,p}}{Y}\right) \geq \frac{1}{fu_p}$ from equation 4. Ka_{AP} and Ka_{PR} in term 3, are
134 deconvolved from expressions for partitioning into RBCs or plasma lipids ($f_{NL,RBC}$ and $f_{NP,RBC}$, or $f_{NL,p}$ and $f_{NP,p}$)
135 and interactions with RBCs acid phospholipids or plasma proteins (5, 8). Therefore, Ka_{AP} and Ka_{PR} might be
136 negligible or even become zero when partitioning into RBCs or plasma lipids determine fu_p and BP regardless
137 of LogP: Kpu_{RBC} and subsequently $Ka_{AP} = 0$ if $BP = 1$ -Haematocrit; and $Ka_{PR} = 0$ if $fu_p = 1$.

138

139 Finally, the plasma Vss can be calculated using the predicted Kpu values as follows (Eq.6):

$$Vss = \sum ((Kpu_i \cdot fu_p) \cdot V_{tissue,i} \cdot (1 - E_i)) + Kpu_{RBC} \cdot fu_p \cdot V_{RBC} + V_{plasma} \quad (6)$$

140 where E_i and $V_{tissue,i}$ represents respectively the extraction ratio and the volume of i^{th} tissue (values used are given
141 in Table S1). V_{RBC} is the volume of red blood cells. V_{plasma} is the plasma volume, and $V_{plasma} = 3.15L$ for a reference

142 man of 70 kg (9). The tissue volume V_{tissue} was calculated as a fraction of body weight (BW) corrected by the
143 tissue density (kg/L): $V_{\text{tissue}} = f_{\text{BW}} \times \text{BW}/\text{density}$.

144

145 Global sensitivity analysis on drug parameters: PRCC

146 Global sensitivity analyses (GSA) use a set of samples representative of the parameter space of inputs to
147 explore the design space which are simulated according to their distribution functions and possible correlations
148 (24). Monte Carlo sampling of input parameters generates output variable distributions to be used in assessing
149 model uncertainty (25). Based on Monte Carlo simulations, scatterplots of the tissue Kpus predicted from the
150 R&R model and each drug parameter were generated in order to identify visually the relationships between the
151 inputs and outputs (tissue Kpus) which were all monotonic and mostly nonlinear (Figures S1-S4).

152 Partial rank correlation coefficient (PRCC) is a method for GSA based on rank-transformed linear
153 regression analysis. It is a powerful method to evaluate the statistical input-output relationships after eliminating
154 the linear influence of other input variables and when there is a nonlinear monotonic trend between input
155 parameters and output variables as it requires a non-parametric test of ranked data (25). It has been
156 demonstrated that for nonlinear non-monotonic trends, PRCC does not perform as well as variance-based
157 methods, such as extended Fourier Amplitude Sensitivity Test (eFAST). Nevertheless, when applied to monotonic
158 trends, combining Latin hypercube sampling (LHS) (26, 27) with PRCC this methods is robust, reliable and less
159 computationally costly (28). Additionally, PRCC can also consider interactions between parameters (29).
160 Calculated PRCC is a standardised similar sensitivity measure between -1 and 1 that can be compared among
161 different parameters, with a value of $|PRCC|$ close to 1 indicating the parameter has a strong impact on the
162 model output. Sensitivity of Kpu predictions to the physicochemical input parameters, *i.e.* LogP, pKa, f_{up} and BP,
163 were investigated for hypothetical but relevant neutral, acid, weak basic and moderate-to-strong basic
164 compounds in R v.3.4.2 with Rstudio v.1.0.153 (30). Zwitterions and multiple charged compounds were not
165 explicitly considered in this work as in the R&R model they are expected to behave like strong bases or
166 acids/weak bases depending primarily on their most basic/acidic pKa value. For each drug class, a total of 10,000
167 compounds with different properties were generated by LHS with the R package "lhs" (31). Each simulated set
168 of compounds per drug class were uniformly sampled by selecting values for each physicochemical drug input
169 parameter from the ranges specified in Table I. The ranges represent realistic intervals for the drug-dependent
170 parameters (32, 33). For each simulated compound, tissue Kpu values were then calculated using the R&R
171 equations 1 and 2. The input parameter (drug physicochemical properties) and output parameter (tissue Kpu)
172 values were transformed into their ranks and PRCCs were calculated following the procedure described
173 previously (28). The significance of a non-zero PRCC value was tested using a two-sided Student's t test (28) as

174 the number of tests performed is large, a Bonferroni multiple test correction was used (34). Details of the PRCC
175 analysis are provided in Supplemental 1.

176

177 **Relationship between LogP and f_{u_p}**

178 Model input variables are typically assumed to be independent for practical reasons, as non-independent
179 inputs samples are more complex to generate and may need a very large sample size to compute accurate
180 sensitivity measures. However, the assumption of independence among input variables may not be appropriate
181 given the nature of the relationship between, for instance, lipophilicity and plasma protein binding (35-37).
182 Consequently, several degrees of dependency between LogP and f_{u_p} were considered when sampling the LogP
183 and f_{u_p} values:

- 184 1) Independence of LogP and f_{u_p} : LogP and f_{u_p} were each sampled independently from its defined uniform
185 distribution with the LHS method.
- 186 2) A linear relationship between LogP and f_{u_p} while investigating different correlation coefficient $\rho = -0.3, -$
187 0.5 and -0.9 following Iman and Conover's procedure (38).
- 188 3) A nonlinear empirical relationship between LogP/LogD and f_{u_p} ($\rho = -0.8$ for neutral basic drugs, $\rho = 0.5$ for
189 acids) with added noise (35, 39).

190 The sample size of the GSA for the different degrees of dependency evaluated was chosen to be the same
191 ($N=10,000$). Further details regarding the set-up of the dependency between LogP and f_{u_p} are provided in
192 Supplemental 2.

193

194 **Local sensitivity analysis of drug parameters with Vss output**

195 Preliminary analyses based on Monte Carlo sampling of input parameters revealed that the relationship
196 between the drug input parameters and K_p and V_{ss} was not strictly monotonic (data not shown), a key
197 prerequisite for the use of PRCC. Consequently, this type of analysis is inappropriate for investigating the
198 influence of drug input parameters on V_{ss} output. Alternatively, local sensitivity analyses (SA) were performed
199 investigating how small changes in one parameter value at a time affect the model output. The sensitivity
200 coefficient (S_{ij}) for a definite independent variable X were calculated (equation 7) based on the partial
201 differentiation of each output of interest with respect to each model input parameter (40) and normalised by
202 both the output and input parameter to remove the influence of units. (25). S_{ij} quantifies the relative change of
203 the model output at a relative change of the input parameter (Eq.7). It should be noted that each input parameter
204 is perturbed to a small extent while holding all other parameters fixed.

$$S_{ij} = \frac{\partial Y_i}{\partial X_j} \times \frac{X_j}{Y_i} \quad (7)$$

205 where Y_i is the model output i, X_j is the input parameter j.

206 As drug input parameters influence Kpu and subsequently Vss predictions, a local SA of the R&R model
207 was carried out with the most and least influential drug input parameters found from the GSA for each drug class
208 to assess their impact on Vss. Indeed, some tissues have a small physical volume and therefore may become
209 negligible contributors to Vss sensitivity despite having sensitive Kpu values. On the other hand, other tissues
210 can have a large volume and not sensitive Kpu values but be very influential on Vss. Additionally, tissues with a
211 high drug extraction ratio (close to 1) may have a low influence on Vss. The sensitivity coefficients depend on the
212 specific set of parameter values used and the ranges of the input variable were selected to be the same as the
213 ones used in the GSA (Table I). This analysis was not meant to be exhaustive and to investigate all possible
214 scenarios. As such, cases of a high lipophilicity-high protein bound compound ($\text{LogP}=3$, $f_{\text{p}}=0.01$) and a low
215 lipophilicity-low protein bound compound ($\text{LogP}=-0.3$, $f_{\text{p}}=0.9$) were investigated to illustrate the impact on drug
216 types frequently encountered during drug discovery and development that can influence significantly drug
217 distribution.

218

219 Incorporation of uncertainties in physiological parameters

220 Tissue composition data originates from a very limited number of studies. This section investigated how
221 uncertainties in tissue composition data may propagate into Kpu and Vss predictions. The term uncertainty
222 includes both biological variability (different sources/animals used to generate the data) and analytical
223 uncertainty. Physiological input parameters for PBPK models especially tissue composition data are generally
224 fixed to average values obtained from the literature (Tables S2 and S3) (5, 8, 41, 42). However, most studies that
225 focused on collection of human and rat tissue composition data (*i.e.*, interstitial, intracellular, and vascular
226 volumes, albumin and lipoprotein concentrations) reported uncertainties in those measurements (43-48). The
227 reported coefficients of variation (CV) varied widely from 2% to 66% depending on the fractional tissue volume
228 but measurements were often very sparse, with only one individual measurement reported in certain cases.
229 Measurements could also be inaccurate due to experimental limitations. Tissue composition data uncertainty
230 can also be due to data arising from subjects of differing ages, races/strains, weights and sex. Additionally, all
231 physiological parameters are associated with inherent biological variability in a population (animal or human).
232 Uncertainties are generally not explicitly incorporated in Kpu predictions. Therefore, parameter uncertainty and
233 variability in tissue compositions values could have an influence on the accuracy of Kpu and therefore the
234 accuracy of Vss predictions. The sensitivity of physiological parameters on drug distribution was explored by
235 incorporating 30% uncertainty on the following set of input parameters in equations 1 and 2: f_{NL} , f_{NP} , f_{IW} , f_{EW} ,
236 $[\text{AP}]_T$, $[\text{AP}]_{\text{RBC}}$, $[\text{PR}]_T/[\text{PR}]_p$. Three scenarios were investigated which included 30% uncertainty on different terms
237 of the equation: (i) all tissue fractions (f_{NL} , f_{NP} , f_{IW} , f_{EW}), acidic phospholipids ($[\text{AP}]_T$, $[\text{AP}]_{\text{RBC}}$) and protein ratios

238 ([PR]_T/[PR]_p); (ii) all tissue fractions only; and (iii) acidic phospholipids and protein ratios only. This analysis served
239 to identify the most influential physiological parameter(s). Distributions of fractional tissue volumes had mean
240 values matching the typical average values used for tissue composition based models (42) and a CV of 30 % were
241 generated.

242 The tissue fractions were assumed to follow logistic-normal distributions to constrain the values between
243 0 and 1 (49). For this, the j normalised fractional tissue volumes per tissue were assumed to follow a (j+1)-
244 dimensional logistic-normal distribution which is derived after the transformation of a standard (j+1)-
245 multivariate normal distribution with mean vector M and variance-covariance matrix Σ. Examples of how to
246 generate samples from a logistic-normal distribution were previously reported (49, 50). It was assumed that F =
247 $[f_1, f_2, \dots, f_j]^T \sim N_j(M, \Sigma)$, where F is a j-dimensional vector that follows a standard multivariate normal distribution
248 with mean vector M defined as a null-vector of length j, and variance-covariance matrix Σ defined as a j-diagonal
249 matrix of 0.0862 (=0.30² in order to have 30 % CV). For plasma, the two normalised fractional parameters (f_{NP}
250 and f_{NL}) were assumed to follow a two-dimensional logistic normal distribution, whereas for adipose, bone, brain,
251 gut, heart, kidney, liver, lung muscle, skin, and spleen, four normalised fractional parameters (f_{NP} , f_{NL} , f_{EW} and f_{IW})
252 were assumed to follow a four-dimensional logistic normal distribution. For blood cells, the three normalised
253 fractional parameters (f_{NP} , f_{NL} , and f_{IW}) were assumed to follow a three-dimensional logistic normal distribution.
254 Here, M and Σ parameters were fixed to generate population distributions of fractional tissue volumes that have
255 means matching the average physiological parameter values (42) and a CV of 30% in the logistic domain. On the
256 other hand, $[AP^-]_T$, $[AP^-]_{RBC}$, $[PR]_T/[PR]_p$ were sampled from a normal distribution ($N(\mu, \sigma)$) where μ is the average
257 value given and σ is the variance of the associated normal in order to generate distributions of these physiological
258 parameters with mean matching the average values and a CV of 30%. Additional details of the incorporation of
259 uncertainties are provided in Supplemental 3.

260 Finally, Kpu values were estimated based on R&R equations (Eq. 1 and 2) for a hypothetical compound
261 of each class (neutral, acid, weak base, strong base) under the three different correlation assumptions outlined
262 above. Additionally, the analysis was done according to four case scenarios of LogP and f_{UP} which corresponded
263 to: a hydrophilic, a lipophilic, a highly bound and a lowly bound compound. These cases represented examples
264 frequently encountered during drug development (Table II). Simulations of fractional tissue volumes, $[AP^-]_T$,
265 $[AP^-]_{RBC}$ and $[PR]_T/[PR]_p$ ratios (N=1000 each) and calculation of Kpu and Vss values for each set of simulated
266 tissue composition values (Eq.1,2, and 6) were implemented in R. We defined the effect of uncertainties in input
267 on output as very influential if the CV% on the output was greater than 10% for a 30 CV% of the input.

268

269 **Results**270 **Global sensitivity analysis of drug-specific parameters: PRCC**

271 The drug-specific input parameters used for the K_{pu} predictions were pKa, LogP, f_{u,p} and BP, depending
272 on drug class (Eq. 1 and 2). The results of GSA combining LHS and PRCC with the different relationships between
273 LogP and f_{u,p} investigated are summarised in Table III. The interpretation of the results depended on the sampled
274 input space and on the correlation between LogP and f_{u,p} parameters. However, all parameters were influential
275 and showed statistically significant PRCC values (p-value<0.001 after Bonferroni correction) except for pKa for
276 adipose and skin K_{pus} for weak bases (Figure S6).

277 When all input parameters were sampled independently, the PRCCs assessment showed that LogP
278 played a major role in the K_{pu} predictions for all drug classes, indicating generally the highest sensitivity of all
279 input parameters (Figure 1). The second most influential parameter overall was f_{u,p}. For acidic drugs, it was even
280 the most influential parameter for a few of the tissue K_{pus} (heart, kidney, lung and skin) which represented
281 tissues with a high fractional volume of extracellular water and albumin ratio (Figure 1). For strong bases, f_{u,p} was
282 actually the most influential input parameter for most K_{pus} except for the tissues that displayed the smallest
283 tissue concentration of AP, namely adipose, bone and brain, where LogP was the most influential input
284 parameter. For strong bases, BP was found to have a strong impact on the tissue K_{pu} outputs (Figure 1). In
285 general, among the investigated parameters, pKa tended to be the least influential parameter with absolute
286 PRCC values between 0.18 and 0.72 for acids and strong bases during independent sampling of LogP and f_{u,p}. In
287 general, LogP, pKa and BP were generally positively correlated with the K_{pu} outputs across all classes except for
288 the strong bases where pKa was negatively correlated with the outputs (Figure S6). On the other hand, f_{u,p} was
289 strongly negatively correlated with the outputs across all drug classes (Figures S5 and S6).

290 When considering a low to moderate correlation of $\rho = -0.3$ or -0.5 between LogP and f_{u,p}, the results
291 were similar to the ones obtained where LogP and f_{u,p} were independent, where the sensitivity of K_{pu} to LogP
292 was the highest followed by f_{u,p} and pKa (Figure 1-Figure 2). However, for acids, f_{u,p} became a more influential
293 parameter for some of the tissue K_{pus} although the difference between the PRCC values of LogP and f_{u,p} of these
294 tissues were actually slight (PRCC < 0.1) (Figure S5). For strong bases, BP became a more influential parameter
295 than f_{u,p} for a majority of the tissue K_{pus} (maximal PRCC of |0.79|, Figure 1).

296 When considering a strong correlation of $\rho = -0.9$, a minimal change was observed for neutral and weak
297 basic compounds where LogP remained the most sensitive parameter (Figure 1-Figure 2). For acidic compounds,
298 LogP now had the smallest PRCCs (between 0.49 and 0.69, Figure 1). For strong bases, BP was now the most
299 sensitive parameter (PRCC between 0.74 and 0.84), followed by f_{u,p} (PRCC between -0.56 and -0.72), LogP (PRCC
300 between 0.02 and 0.34) and pKa (PRCC between -0.04 and -0.31) (Figure 2). When considering a nonlinear
301 relationship where f_{u,p} was considered dependent on LogP, sensitivity ranking was similar to when considering a

302 strong correlation of -0.9 between LogP and f_{u_p} . The exception was for acids where f_{u_p} was the most influential
303 parameter (PRCC between -0.76 and -0.92, Figure 1). It appeared that a nonlinear relationship where f_{u_p}
304 depended on LogP, the distribution of f_{u_p} was mostly concentrated around its lower range (more than 60% of
305 simulated compounds had an $f_{u_p}<0.1$) while with a correlation of -0.9 f_{u_p} stayed uniformly distributed within the
306 whole defined range.

307

308 **Local sensitivity analysis with Vss output**

309 Drug input parameters influenced K_{pu} and subsequently V_{ss} predictions. Figure 3A and Figure 3B
310 illustrated the influence of these least and most influential parameters, respectively, on a normalised score of
311 the V_{ss}. For this assessment, two prototypical compounds, one **high lipophilicity-high protein bound (LogP=3,**
312 **$f_{u_p}=0.01$**) and one **low lipophilicity-low protein bound (LogP=-0.3, $f_{u_p}=0.9$)** compound were investigated.

313 Although pKa for acids, strong and weak bases and f_{u_p} for neutrals were identified as the least relevant, these
314 parameters still had an important influence on the V_{ss} predictions, especially between pKa of 5 and 9 where
315 acids, strong and weak bases can be ionised at physiological pH and when plasma protein binding was high (f_{u_p}
316 <0.1) as it has an inverse influence on tissue K_{pu} (Figure 3). For neutrals, an increase in sensitivity of V_{ss} was
317 observed when f_{u_p} approached 1; when considering a lipophilic compound with LogP=3, the most apparent
318 change was seen between f_{u_p} 0.001 and 0.1 while for a hydrophilic compound with LogP=-0.3, it was between
319 0.9 and 1. In this latter case of high f_{u_p} , K_{PR} was set to zero as negative values were obtained (9), term 2 became
320 zero in Equation 2, and term 3 (function of LogP and pKa) was dominant in K_{pu} predictions resulting in a sudden
321 change in V_{ss} and a sharp profile. For acidic compounds, a positive change in the V_{ss} was observed from pKa
322 values ranging from 2 to 7.2 approximately, and negative change for pKa values between 7.2 to 8 for compounds
323 with high and low lipophilicity although the normalised sensitivity coefficient at pKa 7.2 was around 6 for
324 lipophilic acidic compound and only 2.2 for hydrophilic acidic compound. No change in V_{ss} was observed for
325 weak bases with pKa values between 3 and 5 where compounds are mainly unionised (78% with < 5% ionisation
326 in plasma) and a positive change was observed from a pKa of 5 to 6.9 for an unbound hydrophilic weakly basic
327 compound, while a negative change was observed for a bound lipophilic weak basic compound. In this latter case,
328 lipid partitioning was greater than nonspecific protein binding (e.g., low f_{u_p} relative to LogP), the terms 1 and 3
329 became negligible in Eq. 2 and the term 2 (dependent on a mixture of LogP, pKa, f_{u_p}) was predominant and
330 decreased as pKa increased. For strong basic compounds, negative change in the V_{ss} was observed from pKa 7
331 to 7.5, a positive change was observed from pKa 7.5 to 10, and no change from pKa 10 to 11 (fully ionised from
332 pKa > 9.5); the normalised sensitivity coefficient at pKa 7.5 was -1.5 for free hydrophilic strongly basic compounds
333 and only -0.3 for bound lipophilic strongly basic compound. In this latter case, the affinity constant K_{AP} varied
334 greatly as K_{pu,RBC} was very high (Eq. 1) causing a higher change in V_{ss}.

335 Compared to Figure 3A, the normalised local sensitivity values of Vss to the most influential drug
336 parameters axis in Figure 3B were indeed larger corroborating that the parameters LogP and BP were
337 considerably more influential. For a strongly basic compound with $pK_a=8$, $\text{LogP}=-0.3$ and $f_{u_p}=0.9$ (high f_{u_p}), $K_{a_{AP}}$
338 was set to zero as negative values were obtained when $BP < f_{u_p}$; consequently term 2 became null in Equation 1,
339 and term 3 (function of LogP and pK_a which were fixed) was dominant in Kpu predictions 1 resulting in no change
340 in Vss and then a sharp profile when $BP > f_{u_p}$.

342 Incorporation of uncertainties in tissue composition parameters

343 The impact of uncertainties in tissue composition input data on Vss predictions is illustrated in Figure 4 and
344 the individual results of all tissue Kpu outputs can be found in Figure S7. For all compound classes, the effect of
345 tissue composition data on model output (Kpu and Vss) was influential as the CV varied up to 43% in Kpu outputs
346 and up to 32% in Vss outputs when considering a CV of 30% in tissue composition. In order to identify which
347 parameter was primarily responsible for the observed changes and sensitivities, three scenarios were
348 investigated.

349 Firstly, uncertainties of 30% in all tissue composition parameters resulted in the highest output variability for
350 highly bound strong bases ($f_{u_p}<0.01$) with output CVs between 25 and 45% and between 25 and 32%,
351 respectively, for Kpu and Vss (solid lines, Figure 4C). The CV values in output parameters greater than 30%
352 resulted from the variability of AP being included at the level of the tissue $[AP^-]_T$ and of the red blood cell values
353 $[AP^-]_{RBC}$ in Eq. 1 and 3 leading to a ratio of $[AP^-]_T/[AP^-]_{RBC}$ with $CV\%>30$ for Kpu outputs (e.g., 41%CV for Kpu lung,
354 48%CV for Kpu skin). For unbound strong bases in plasma ($f_{u_p}>0.9$, Figure 4D) and other compound classes, the
355 influence of uncertainties in tissue compositions on Kpu and Vss outputs was smaller but still influential with CVs
356 between 10 and 30%, and 9 and 21% for Kpu and Vss, respectively (solid lines, Figure 4D).

357 Secondly, uncertainties of 30% in fractional tissue volumes only resulted in limited output variability with
358 CV of 0 to 30 % for both Kpu and Vss parameters (dashed lines, Figure 4). For the tissue volumes to be influential,
359 the specific and nonspecific binding of drug needed to be negligible (*i.e.*, high f_{u_p} and low LogP). As specific and
360 nonspecific binding increased, the relevance of the fractional volume terms diminished (Eq. 1 and 2) since they
361 represented only a small proportion of the total tissue volumes. It should be noted that the adipose Kpu stood
362 out in its behavior compared to the other tissues, probably because of the high fractional volume of neutral lipids
363 compared to other tissues (Figure S7A and B). When varying LogP for strong bases at an f_{u_p} of 0.9, adding
364 uncertainties in fractional tissue volumes had an impact on tissue Kpus with CVs between 5 and 28% (dashed
365 lines, Figure 4) but resulting in a CV of 16% in Vss predictions possibly due to the errors cancelling each other out
366 (Figure 4D).

367 Finally, uncertainties of 30% in only $[AP]_T$, $[AP]_{RBC}$ and extracellular $[PR]_T/[PR]_p$ resulted in similar output
368 variability of 30% in all tissue composition parameters, especially when f_{up} was low ($f_{up}<0.1$) (solid and dotted
369 lines were blended, Figure 4B), suggesting that uncertainties in tissue AP and extracellular PR levels data
370 dominated the changes in Kpu and Vss outputs in this f_{up} parameter space (an average 43%CV in tissue Kpu and
371 a CV close to 30% in Vss output). Indeed, the term related to AP and K_{AP} in Eq. 1 was set to zero and plasma
372 binding was exclusively driven by nonspecific binding which explained the observed sharp profiles in Figure S7B.

373 Discussion

374 In this paper, global and local SA were conducted to identify the key drug and physiological parameters
375 of tissue distribution based on the mechanistic Kpu equations of R&R (5, 8). These equations were selected as
376 they represent an accurate prediction tool for Kpu values (10) and mechanistically integrate many of the
377 underlying distribution mechanisms along with physiological information. However, a similar analysis is of course
378 applicable to other Kpu mechanistic equations for Kpu predictions as well (4, 7, 51-54). The decomposition of
379 equations 1 and 2 into three terms in the Methods section allowed a better understanding of the equations and
380 how uncertainty propagates into Kpu and Vss when varying drug and tissue composition parameters. However,
381 several key distribution processes are not considered in the R&R model such as tissues being divided into
382 interstitial and intracellular spaces with differing pH values (7), lysosomal trapping (55), microsomal partitioning
383 (56), active transport across membranes (e.g., for poorly permeable molecules) and could contribute to the Vss
384 misprediction.

385 The GSA combining LHS and PRCC was performed on input parameter ranges covering a wide parameter
386 space (Table I) (28) and with several degrees of dependency between LogP and f_{up} . Contradicting reports exist
387 in the literature regarding the relationship (35, 57-61) or lack of relationship (62-64) between f_{up} and LogP (or
388 LogD). Degrees of correlation were selected based on a few nonlinear negative relationships reported in the
389 literature with correlation values ranging from -0.91 to -0.36 depending on the investigated dataset of
390 compounds and classes and also the measured or calculated LogP/LogD term considered (35, 57, 65, 66).
391 Ultimately, the correlation can slightly change the sensitivity ranking of the input parameters especially for acids
392 and strong bases and additional information on correlations between LogP and f_{up} within the specific chemotype
393 could be useful as input for the parameter estimation process for these classes.

394 In the current analysis, different correlations between f_{up} and LogP were investigated and overall two
395 patterns could be distinguished: 1) a case with no-to-moderate extent of correlation and 2) a case with high
396 correlation (Table III). When all input parameters were assumed to be independent, LogP was generally the most
397 influential parameter for neutral drugs and weak bases which were predominantly unionised at physiological pH;
398 while f_{up} was the most influential input parameter for most Kpus for strong bases. Given its considerable
399 importance, any errors in computational or experimental LogP determination can significantly influence Kpu
400 predictions (Figure 1). A recent study showed that among different LogP methods investigated, the LogP
401 prediction of the best model against a compound dataset representing pharmaceutical space was within one log
402 unit approximately 70% of the time (67). Introducing a correlation between LogP and f_{up} constrained the
403 sampling space and made it less likely that term 2 of equations 1 and 2 became zero, therefore term 3 became
404 the only relevant mechanism of tissue partitioning. This attenuated the importance of LogP especially for acids
405 and strong bases. A correlated sample may be a more plausible combination of drug input parameters and

406 possibly a better representation of the behaviour of drug compounds when correlations are known (68, 69).
407 However, when LogP was uniformly sampled and f_{u_p} was calculated using Yamazaki *et al.*'s relationship (35), the
408 main limitation was that many of the simulated compounds had a very small f_{u_p} value (<0.05). This may be an
409 artefact caused by the large experimental errors of the drugs as the data were compiled from many different
410 sources (70). Free fraction can be accurately measured up to 0.1% (0.001) for highly bound compounds and
411 becomes more uncertain below this value (71). As f_{u_p} was identified as a highly influential parameter, uncertainty
412 in its determination are likely going to contribute significantly in the variability of Kpu and Vss outputs.

413 PRCC analyses only gave ranking of parameter relevance for Kpu values, but did not evaluate the
414 contribution of each input to the output uncertainty. Other GSA methods including screening methods, variances
415 could be applied although they are more computationally intensive and the interpretation is difficult in the
416 presence of statistical dependence between inputs (72, 73). In contrast to GSA, the local SA assesses the impact
417 of single parametric perturbations on the model output (Kpus, Vss). Although the GSA ranking differed from the
418 local SA ranking in certain parameter spaces, this should not be considered inconsistent as they arise from
419 different design and purposes. The local SA on Vss predictions showed that even the least influential drug
420 parameters (based on PRCC) on Kpu were found to have a relevant influence on the Vss predictions. Particularly
421 when pKa was around physiological pH where acid, weak and strong bases are unionised and as when plasma
422 protein binding was high ($f_{u_p} < 0.1$) (9). On the other hand, the high sensitivity of Kpu and subsequently Vss to BP
423 illustrates how important it is to measure this value for strong basic compounds as BP serves as surrogate for
424 drug interaction with AP in the body (Eq.3). Therefore, when BP is frequently assumed to be one for strong bases
425 due to unavailable measurements, it can actually lead to errors in AP drug affinity calculations and subsequent
426 Kpu and Vss predictions.

427 Due to the lack of tissue composition data in human especially regarding concentrations of AP, albumin
428 and lipoprotein ratios, rat data are used instead (9, 42). However, prediction success of human Vss might be
429 affected by the assumption that rat and human tissue compositions are the same. Our uncertainty analysis
430 illustrated the influence of uncertainties in tissue composition data (*i.e.*, tissue fractions, phospholipids and
431 protein ratios) on Kpu and Vss predictions when a CV of 30% was considered for the tissue composition values.
432 The choice of CV 30% was a realistic average value as a 5 or 15 CV % had been reported for several fractional
433 tissue volumes and up to 60% for other fractional volumes in rat and human (43-46, 74). However, this may
434 inadequately represent the variability in tissue composition in the general population as a large interspecies
435 variation can exist in these measured parameters. For example, a fractional AP content of 0.0004 was found in
436 rat brain, whereas a content of 0.02 was found in human brain (75). Moreover, lipid composition of neutral lipids
437 and acidic phospholipids was shown to differ between species, especially compositions of fatty acids (74, 76),
438 which may lead to variable interactions with drugs from one species to another. Alternatively, modelling and

439 simulations in conjunction with imaging techniques (e.g., MRI, PET, PET-CT scan) can be used to help characterise
440 tissue distribution in the body and different tissues (77-79).

441 Uncertainties in tissue composition are likely going to have a considerable impact on the success of V_{ss}
442 predictions for all classes and especially for strong bases with low f_{u,p} mostly due to the uncertainty in data on
443 tissue specific acidic phospholipid and protein levels. Further examination by separation of fractional tissue
444 volumes from [AP⁻] or extracellular PR revealed that fractional tissue volumes had less impact than AP and
445 extracellular PR exception for a compound with high LogP and f_{u,p} (Figure 4). Overall, this uncertainty analysis
446 indicates that additional research and a better characterisation of AP and extracellular PR (albumin and
447 lipoprotein) levels in tissues and plasma would improve the confidence in K_{pu} and V_{ss} prediction accuracies
448 across species. However, it should be noted that this assessment is based on the R&R model, which assumes that
449 ionised bases interact predominately with AP and uncharged with neutral phospholipids and neutral lipids. This
450 assumption has been questioned recently (80, 81). In addition to model refinements, additional data particularly
451 AP and extracellular PR in the different tissues will help to reduce uncertainty and obtain more reliable K_{pu}
452 predictions in the future.

453 Finally, for the parameter estimation process, less influential parameters for K_{pu} predictions in each drug
454 class might be assigned fixed values depending on the sensitivity of the parameter space, while influential
455 parameters could be fitted using priors and uncertainty associated with experimental methods and data. In this
456 work, we found that the sensitivity ranking depends on the degree of dependence between LogP and f_{u,p} for
457 acids and strong bases, therefore this needs to be taken into account when fixing certain parameters.

458 **Conclusions**

459 Based on the GSA using a wide range of drug input parameters, the most influential parameters on K_{pu}
460 predictions in the R&R model, were generally LogP and f_{u,p} for the drug-specific parameters.
461 Uncertainties in tissue composition have a considerable influence on K_{pu} and V_{ss} predictions for all classes and
462 especially for strong bases with low f_{u,p} mostly due to the uncertainty in data on tissue specific acidic phospholipid
463 and protein levels.
464 In the context of parameter estimation for PBPK models and dimensionality reduction, less influential
465 parameters for K_{pu} predictions in each drug class might be assigned fixed values depending on the sensitivity of
466 the parameter space, while influential parameters could be fitted, for instance using a Bayesian approach, where
467 priors and uncertainty associated with experimental methods and data are accounted for.

- 468 **References**
- 469 1. Jones HM, Chen Y, Gibson C, Heimbach T, Parrott N, Peters SA, et al. Physiologically based
470 pharmacokinetic modeling in drug discovery and development: a pharmaceutical industry perspective. *Clin
471 Pharmacol Ther.* 2015;97(3):247-62. doi: 10.1002/cpt.37.
- 472 2. Jamei M. Recent Advances in Development and Application of Physiologically-Based Pharmacokinetic
473 (PBPK) Models: a Transition from Academic Curiosity to Regulatory Acceptance. *Curr Pharmacol Rep.*
474 2016;2:161-9. doi: 10.1007/s40495-016-0059-9.
- 475 3. Luzon E, Blake K, Cole S, Nordmark A, Versantvoort C, Berglund EG. Physiologically based
476 pharmacokinetic modeling in regulatory decision-making at the European Medicines Agency. *Clin Pharmacol
477 Ther.* 2016. doi: 10.1002/cpt.539.
- 478 4. Poulin P, Theil FP. A Priori Prediction of Tissue:Plasma Partition Coefficients of Drugs to Facilitate the
479 Use of Physiologically-Based Pharmacokinetic Models in Drug Discovery. *Journal of Pharmaceutical Sciences.*
480 2000;89(1):16-35. doi: 10.1002/(sici)1520-6017(200001)89:1<16::aid-jps3>3.0.co;2-e.
- 481 5. Rodgers T, Leahy D, Rowland M. Physiologically based pharmacokinetic modeling 1: predicting the
482 tissue distribution of moderate-to-strong bases. *J Pharm Sci.* 2005;94(6):1259-76. doi: 10.1002/jps.20322.
- 483 6. Berezhkovskiy LM. Volume of distribution at steady state for a linear pharmacokinetic system with
484 peripheral elimination. *Journal of Pharmaceutical Sciences.* 2004;93(6):1628-40. doi: DOI 10.1002/jps.20073.
- 485 7. Schmitt W. General approach for the calculation of tissue to plasma partition coefficients. *Toxicol In
486 Vitro.* 2008;22(2):457-67. doi: 10.1016/j.tiv.2007.09.010.
- 487 8. Rodgers T, Rowland M. Physiologically based pharmacokinetic modelling 2: predicting the tissue
488 distribution of acids, very weak bases, neutrals and zwitterions. *J Pharm Sci.* 2006;95(6):1238-57. doi:
489 10.1002/jps.20502.
- 490 9. Rodgers T, Rowland M. Mechanistic approaches to volume of distribution predictions: understanding
491 the processes. *Pharm Res.* 2007;24(5):918-33. doi: 10.1007/s11095-006-9210-3.
- 492 10. Graham H, Walker M, Jones O, Yates J, Galetin A, Aarons L. Comparison of in-vivo and in-silico methods
493 used for prediction of tissue: plasma partition coefficients in rat. *J Pharm Pharmacol.* 2012;64(3):383-96. doi:
494 10.1111/j.2042-7158.2011.01429.x.
- 495 11. Jones RD, Jones HM, Rowland M, Gibson CR, Yates JW, Chien JY, et al. PhRMA CPCDC initiative on
496 predictive models of human pharmacokinetics, part 2: comparative assessment of prediction methods of
497 human volume of distribution. *J Pharm Sci.* 2011;100(10):4074-89. doi: 10.1002/jps.22553.
- 498 12. Woodruff TJ, Bois FY. Optimization issues in physiological toxicokinetic modeling: a case study with
499 benzene. *Toxicol Lett.* 1993;69(2):181-96.
- 500 13. Yang J, Jamei M, Heydari A, Yeo KR, de la Torre R, Farre M, et al. Implications of mechanism-based
501 inhibition of CYP2D6 for the pharmacokinetics and toxicity of MDMA. *J Psychopharmacol.* 2006;20(6):842-9.
502 doi: 10.1177/0269881106065907.
- 503 14. Peters SA. Identification of intestinal loss of a drug through physiologically based pharmacokinetic
504 simulation of plasma concentration-time profiles. *Clinical Pharmacokinetics.* 2008;47(4):245-59. doi: Doi
505 10.2165/00003088-200847040-00003.
- 506 15. Xia B, Heimbach T, Gollen R, Nanavati C, He H. A simplified PBPK modeling approach for prediction of
507 pharmacokinetics of four primarily renally excreted and CYP3A metabolized compounds during pregnancy.
508 *AAPS J.* 2013;15(4):1012-24. doi: 10.1208/s12248-013-9505-3.
- 509 16. Ke A, Barter Z, Rowland-Yeo K, Almond L. Towards a Best Practice Approach in PBPK Modeling: Case
510 Example of Developing a Unified Efavirenz Model Accounting for Induction of CYPs 3A4 and 2B6. *CPT
511 Pharmacometrics Syst Pharmacol.* 2016;5(7):367-76. doi: 10.1002/psp4.12088.
- 512 17. Budha NR, Ji T, Musib L, Eppler S, Dresser M, Chen Y, et al. Evaluation of Cytochrome P450 3A4-
513 Mediated Drug-Drug Interaction Potential for Cobimetinib Using Physiologically Based Pharmacokinetic
514 Modeling and Simulation. *Clin Pharmacokinet.* 2016;55(11):1435-45. doi: 10.1007/s40262-016-0412-5.

- 515 18. Tsamandouras N, Rostami-Hodjegan A, Aarons L. Combining the 'bottom up' and 'top down'
516 approaches in pharmacokinetic modelling: fitting PBPK models to observed clinical data. Br J Clin Pharmacol.
517 2015;79(1):48-55. doi: 10.1111/bcp.12234.
- 518 19. European Medicines Agency, Guideline on the qualification and reporting of physiologically based
519 pharmacokinetic (PBPK) modelling and simulation. 2018 [May 2019]; Available from:
520 [https://www.ema.europa.eu/en/documents/scientific-guideline/guideline-reporting-physiologically-based-](https://www.ema.europa.eu/en/documents/scientific-guideline/guideline-reporting-physiologically-based-pharmacokinetic-pbpk-modelling-simulation_en.pdf)
521 [pharmacokinetic-pbpk-modelling-simulation_en.pdf](https://www.ema.europa.eu/en/documents/scientific-guideline/guideline-reporting-physiologically-based-pharmacokinetic-pbpk-modelling-simulation_en.pdf).
- 522 20. U.S. Food and Drug Administration, Physiologically Based Pharmacokinetic Analyses — Format and
523 Content : Guidance for Industry. 2018 [May 2019]; Available from:
524 <https://www.fda.gov/downloads/Drugs/GuidanceComplianceRegulatoryInformation/Guidances/UCM531207.pdf>.
- 526 21. Graham H. Predicting drug distribution in rat and human: University of Manchester; 2012.
- 527 22. Davies B, Morris T. Physiological parameters in laboratory animals and humans. Pharm Res.
528 1993;10(7):1093-5.
- 529 23. Rowland M, Tozer TN. Clinical Pharmacokinetics: Concepts and Applications. 3rd ed: Lippincott
530 Williams & Wilkins; 1995.
- 531 24. Kamboj S, Cheng JJ, Yu C. Deterministic vs. probabilistic analyses to identify sensitive parameters in
532 dose assessment using RESRAD. Health Phys. 2005;88(5 Suppl):S104-9.
- 533 25. Hamby DM. A review of techniques for parameter sensitivity analysis of environmental models. Environ
534 Monit Assess. 1994;32(2):135-54. doi: 10.1007/BF00547132.
- 535 26. McKay MD, Beckman RJ, Conover WJ. Comparison of Three Methods for Selecting Values of Input
536 Variables in the Analysis of Output from a Computer Code. Technometrics. 1979;21(2):239-45. doi:
537 10.1080/00401706.1979.10489755.
- 538 27. Blower SM, Dowlatabadi H. Sensitivity and Uncertainty Analysis of Complex-Models of Disease
539 Transmission - an Hiv Model, as an Example. Int Stat Rev. 1994;62(2):229-43. doi: Doi 10.2307/1403510.
- 540 28. Marino S, Hogue IB, Ray CJ, Kirschner DE. A methodology for performing global uncertainty and
541 sensitivity analysis in systems biology. J Theor Biol. 2008;254(1):178-96. doi: 10.1016/j.jtbi.2008.04.011.
- 542 29. Saltelli A, Chan K, Scott EM. Sensitivity analysis. Chichester ; New York: Wiley; 2000.
- 543 30. R Core Team. R: A Language and Environment for Statistical Computing. Vienna, Austria2018.
- 544 31. Carnell R. lhs: Latin Hypercube Samples. R package version 1.0.1 ed: Comprehensive R Archive Network
545 (CRAN); 2019.
- 546 32. Margolskee A, Darwich AS, Pepin X, Pathak SM, Bolger MB, Aarons L, et al. IMI - oral biopharmaceutics
547 tools project - evaluation of bottom-up PBPK prediction success part 1: Characterisation of the OrBiTo database
548 of compounds. Eur J Pharm Sci. 2017;96:598-609. doi: 10.1016/j.ejps.2016.09.027.
- 549 33. Poulin P, Jones HM, Jones RD, Yates JW, Gibson CR, Chien JY, et al. PhRMA CPCDC initiative on
550 predictive models of human pharmacokinetics, part 1: goals, properties of the PhRMA dataset, and comparison
551 with literature datasets. J Pharm Sci. 2011;100(10):4050-73. doi: 10.1002/jps.22554.
- 552 34. Abdi H. The Bonferroni and Šidák Corrections for Multiple Comparisons. Encyclopedia of measurement
553 and statistics. 2007;3.
- 554 35. Yamazaki K, Kanaoka M. Computational prediction of the plasma protein-binding percent of diverse
555 pharmaceutical compounds. J Pharm Sci. 2004;93(6):1480-94. doi: 10.1002/jps.20059.
- 556 36. Laznicka M, Laznickova A. The effect of lipophilicity on the protein binding and blood cell uptake of
557 some acidic drugs. J Pharm Biomed Anal. 1995;13(7):823-8. doi: 10.1016/0731-7085(95)01504-e.
- 558 37. Ghafourian T, Amin Z. QSAR models for the prediction of plasma protein binding. Bioimpacts.
559 2013;3(1):21-7. doi: 10.5681/bi.2013.011.
- 560 38. Iman RL, Conover WJ. A Distribution-Free Approach to Inducing Rank Correlation among Input
561 Variables. Commun Stat B-Simul. 1982;11(3):311-34. doi: Doi 10.1080/03610918208812265.
- 562 39. Saltelli A. Global sensitivity analysis : the primer. Chichester, England ; Hoboken, NJ: John Wiley; 2008.

- 563 40. Saltelli A, Ratto M, Tarantola S, Campolongo F, Commission E, Ispra JRC. Sensitivity analysis practices:
564 Strategies for model-based inference. *Reliab Eng Syst Safe*. 2006;91(10-11):1109-25. doi:
565 10.1016/j.ress.2005.11.014.
- 566 41. Poulin P, Theil FP. Development of a novel method for predicting human volume of distribution at
567 steady-state of basic drugs and comparative assessment with existing methods. *J Pharm Sci*. 2009;98(12):4941-
568 61. doi: 10.1002/jps.21759.
- 569 42. Poulin P, Jones RD, Jones HM, Gibson CR, Rowland M, Chien JY, et al. PHRMA CPCDC initiative on
570 predictive models of human pharmacokinetics, part 5: prediction of plasma concentration-time profiles in
571 human by using the physiologically-based pharmacokinetic modeling approach. *J Pharm Sci*.
572 2011;100(10):4127-57. doi: 10.1002/jps.22550.
- 573 43. Simon G, Rouser G. Species variations in phospholipid class distribution of organs. II. Heart and skeletal
574 muscle. *Lipids*. 1969;4(6):607-14.
- 575 44. Rouser G, Simon G, Kritchevsky G. Species variations in phospholipid class distribution of organs. I.
576 Kidney, liver and spleen. *Lipids*. 1969;4(6):599-606.
- 577 45. Hof H, Simon RG. Phospholipid content of human and guinea pig muscle: post-mortem changes and
578 variations with muscle composition. *Lipids*. 1970;5(5):485-7.
- 579 46. Diagne A, Fauvel J, Record M, Chap H, Douste-Blazy L. Studies on ether phospholipids. II. Comparative
580 composition of various tissues from human, rat and guinea pig. *Biochim Biophys Acta*. 1984;793(2):221-31.
- 581 47. Miller SP, Zirzow GC, Doppelt SH, Brady RO, Barton NW. Analysis of the lipids of normal and Gaucher
582 bone marrow. *J Lab Clin Med*. 1996;127(4):353-8.
- 583 48. Ellmerer M, Schaupp L, Brunner GA, Sendlhofer G, Wutte A, Wach P, et al. Measurement of interstitial
584 albumin in human skeletal muscle and adipose tissue by open-flow microperfusion. *Am J Physiol Endocrinol
585 Metab*. 2000;278(2):E352-6. doi: 10.1152/ajpendo.2000.278.2.E352.
- 586 49. Aitchison J, Shen SM. Logistic-Normal Distributions - Some Properties and Uses. *Biometrika*.
587 1980;67(2):261-72. doi: Doi 10.2307/2335470.
- 588 50. Tsamandouras N, Wendling T, Rostami-Hodjegan A, Galetin A, Aarons L. Incorporation of stochastic
589 variability in mechanistic population pharmacokinetic models: handling the physiological constraints using
590 normal transformations. *J Pharmacokinet Pharmacodyn*. 2015;42(4):349-73. doi: 10.1007/s10928-015-9418-0.
- 591 51. Berezhkovskiy LM. Determination of volume of distribution at steady state with complete
592 consideration of the kinetics of protein and tissue binding in linear pharmacokinetics. *J Pharm Sci*.
593 2004;93(2):364-74. doi: 10.1002/jps.10539.
- 594 52. Peyret T, Poulin P, Krishnan K. A unified algorithm for predicting partition coefficients for PBPK
595 modeling of drugs and environmental chemicals. *Toxicol Appl Pharmacol*. 2010;249(3):197-207. doi:
596 10.1016/j.taap.2010.09.010.
- 597 53. Poulin P, Haddad S. Advancing prediction of tissue distribution and volume of distribution of highly
598 lipophilic compounds from a simplified tissue-composition-based model as a mechanistic animal alternative
599 method. *J Pharm Sci*. 2012;101(6):2250-61. doi: 10.1002/jps.23090.
- 600 54. Poulin P, Theil FP. Prediction of pharmacokinetics prior to in vivo studies. 1. Mechanism-based
601 prediction of volume of distribution. *J Pharm Sci*. 2002;91(1):129-56.
- 602 55. Assmus F, Houston JB, Galetin A. Incorporation of lysosomal sequestration in the mechanistic model for
603 prediction of tissue distribution of basic drugs. *Eur J Pharm Sci*. 2017;109:419-30. doi:
604 10.1016/j.ejps.2017.08.014.
- 605 56. Holt K, Ye M, Nagar S, Korzekwa KR. Prediction of tissue - plasma partition coefficients using
606 microsomal partitioning: Incorporation into physiologically-based pharmacokinetic models and steady state
607 volume of distribution predictions. *Drug Metab Dispos*. 2019. doi: 10.1124/dmd.119.087973.
- 608 57. Davis AM, Webbom PJ, Salt DW. Robust assessment of statistical significance in the use of
609 unbound/intrinsic pharmacokinetic parameters in quantitative structure-pharmacokinetic relationships with
610 lipophilicity. *Drug Metab Dispos*. 2000;28(2):103-6.
- 611 58. Laruelle M, Slifstein M, Huang Y. Relationships between radiotracer properties and image quality in
612 molecular imaging of the brain with positron emission tomography. *Mol Imaging Biol*. 2003;5(6):363-75.

- 613 59. Laznicek M, Kvetina J, Mazak J, Krch V. Plasma protein binding-lipophilicity relationships: interspecies
614 comparison of some organic acids. *J Pharm Pharmacol.* 1987;39(2):79-83.
- 615 60. Lobell M, Sivarajah V. In silico prediction of aqueous solubility, human plasma protein binding and
616 volume of distribution of compounds from calculated pKa and AlogP98 values. *Mol Divers.* 2003;7(1):69-87.
- 617 61. van de Waterbeemd H, Smith DA, Jones BC. Lipophilicity in PK design: methyl, ethyl, futile. *J Comput
618 Aided Mol Des.* 2001;15(3):273-86.
- 619 62. Kratochwil NA, Huber W, Muller F, Kansy M, Gerber PR. Predicting plasma protein binding of drugs: a
620 new approach. *Biochem Pharmacol.* 2002;64(9):1355-74.
- 621 63. Liu JZ, Yang L, Li Y, Pan DH, Hopfinger AJ. Constructing plasma protein binding model based on a
622 combination of cluster analysis and 4D-fingerprint molecular similarity analyses. *Bioorgan Med Chem.*
623 2006;14(3):611-21. doi: 10.1016/j.bmc.2005.08.035.
- 624 64. Saiakhov RD, Stefan LR, Klopman G. Multiple computer-automated structure evaluation model of the
625 plasma protein binding affinity of diverse drugs. *Perspect Drug Discov.* 2000;19(1):133-55. doi: Doi
626 10.1023/A:1008723723679.
- 627 65. Watanabe R, Esaki T, Kawashima H, Natsume-Kitatani Y, Nagao C, Ohashi R, et al. Predicting Fraction
628 Unbound in Human Plasma from Chemical Structure: Improved Accuracy in the Low Value Ranges. *Mol Pharm.*
629 2018;15(11):5302-11. doi: 10.1021/acs.molpharmaceut.8b00785.
- 630 66. Gleeson MP. Plasma protein binding affinity and its relationship to molecular structure: an in-silico
631 analysis. *J Med Chem.* 2007;50(1):101-12. doi: 10.1021/jm060981b.
- 632 67. Plante J, Werner S. JPlogP: an improved logP predictor trained using predicted data. *J Cheminformatics.*
633 2018;10. doi: ARTN 61

634 10.1186/s13321-018-0316-5.
- 635 68. Doki K, Darwich AS, Achour B, Tornio A, Backman JT, Rostami-Hodjegan A. Implications of
636 intercorrelation between hepatic CYP3A4-CYP2C8 enzymes for the evaluation of drug-drug interactions: a case
637 study with repaglinide. *Br J Clin Pharmacol.* 2018;84(5):972-86. doi: 10.1111/bcp.13533.
- 638 69. Melillo N, Darwich AS, Magni P, Rostami-Hodjegan A. Accounting for inter-correlation between enzyme
639 abundance: a simulation study to assess implications on global sensitivity analysis within physiologically-based
640 pharmacokinetics. *J Pharmacokinet Pharmacodyn.* 2019. doi: 10.1007/s10928-019-09627-6.
- 641 70. Vozeh S, Schmidlin O, Taeschner W. Pharmacokinetic drug data. *Clin Pharmacokinet.* 1988;15(4):254-
642 82. doi: 10.2165/00003088-198815040-00005.
- 643 71. Kalvass JC, Phipps C, Jenkins GJ, Stuart P, Zhang X, Heinle L, et al. Mathematical and Experimental
644 Validation of Flux Dialysis Method: An Improved Approach to Measure Unbound Fraction for Compounds with
645 High Protein Binding and Other Challenging Properties. *Drug Metab Dispos.* 2018;46(4):458-69. doi:
646 10.1124/dmd.117.078915.
- 647 72. Da Veiga S, Wahl F, Gamboa F. Local Polynomial Estimation for Sensitivity Analysis on Models With
648 Correlated Inputs. *Technometrics.* 2009;51(4):452-63. doi: 10.1198/Tech.2009.08124.
- 649 73. Saltelli A, Tarantola S. On the relative importance of input factors in mathematical models: Safety
650 assessment for nuclear waste disposal. *Journal of the American Statistical Association.* 2002;97(459):702-9. doi:
651 10.1198/016214502388618447.
- 652 74. Gray GM, Yardley HJ. Lipid compositions of cells isolated from pig, human, and rat epidermis. *J Lipid
653 Res.* 1975;16(6):434-40.
- 654 75. Ruark CD, Hack CE, Robinson PJ, Mahle DA, Gearhart JM. Predicting passive and active tissue:plasma
655 partition coefficients: interindividual and interspecies variability. *J Pharm Sci.* 2014;103(7):2189-98. doi:
656 10.1002/jps.24011.
- 657 76. Kuksis A. Fatty Acid Composition of Glycerolipids of Animal Tissues. In: Kuksis A, editor. *Fatty Acids and
658 Glycerides.* Boston, MA: Springer US; 1978. p. 381-442.
- 659 77. Ulloa JL, Stahl S, Yates J, Woodhouse N, Kenna JG, Jones HB, et al. Assessment of gadoxetate DCE-MRI
660 as a biomarker of hepatobiliary transporter inhibition. *NMR Biomed.* 2013;26(10):1258-70. doi:
661 10.1002/nbm.2946.

- 662 78. Bergstrom M, Grahnen A, Langstrom B. Positron emission tomography microdosing: a new concept
663 with application in tracer and early clinical drug development. *Eur J Clin Pharmacol.* 2003;59(5-6):357-66. doi:
664 10.1007/s00228-003-0643-x.
- 665 79. Chang YJ, Chang CH, Chang TJ, Yu CY, Chen LC, Jan ML, et al. Biodistribution, pharmacokinetics and
666 microSPECT/CT imaging of ¹⁸⁸Re-bMEDA-liposome in a C26 murine colon carcinoma solid tumor animal
667 model. *Anticancer Res.* 2007;27(4B):2217-25.
- 668 80. Holt K, Nagar S, Korzekwa K. Methods to Predict Volume of Distribution. *Current Pharmacology
669 Reports.* 2019;5(5):391-9. doi: 10.1007/s40495-019-00186-5.
- 670 81. Korzekwa K, Nagar S. On the Nature of Physiologically-Based Pharmacokinetic Models -A Priori or A
671 Posteriori? Mechanistic or Empirical? *Pharm Res.* 2017;34(3):529-34. doi: 10.1007/s11095-016-2089-8.

672

Tables

Table I: Constrained bounds of drug parameters

Input parameters	Neutral	Acid	Weak Base	Strong Base
pKa	-	from 2 to 8	from 3 to 7	from 7 to 11
LogP	from -3 to 6			
fu _p	from 0.001 to 1			
BP	from 0.55 to 2.4			

Table II: Simulation case scenarios investigated using sampled fractional tissue volumes and extracellular proteins levels

Drug characteristics	CASE A	CASE B	CASE C	CASE D
Neutral				
BP:1				
Acid				
pKa:3				
BP:0.55				
Weak Base	LogP: -0.3 fu _p : from 0.001 to 1	LogP:3 fu _p : from 0.001 to 1	LogP: from -0.3 to 3 fu _p :0.01	LogP: from -0.3 to 3 fu _p :0.9
pKa:6.5				
BP:1				
Strong Base				
pKa:9				
BP:1				

Table III: Summary of drug parameter sensitivity and ranking based on the performed GSA

	Independently (or low correlation) sampled LogP and fu _p		Correlation of -0.9 or nonlinear relationship between LogP and fu _p	
	High sensitivity parameter (overall PRCC >0.5)	Low sensitivity parameter (overall PRCC <0.5)	High sensitivity parameter (overall PRCC >0.5)	Low sensitivity parameter (overall PRCC <0.5)
Neutrals	LogP>fu _p		LogP>fu _p	
Acids	LogP>fu _p >pKa		pKa~fu _p >LogP	
Weak bases	LogP>fu _p	pKa	LogP	pKa~fu _p
Strong bases	fu _p > BP~LogP	pKa	BP>fu _p	LogP>pKa

>: greater sensitivity ranking; ~: similar sensitivity ranking

Figures

Figure 1: Parameter ranking determined by the PRCC of tissue K_{pu} for each drug class with different relationships between LogP and fraction unbound in plasma (f_{ub}) for neutral and acidic compounds

rob: rest of body; RBC: Red blood cell

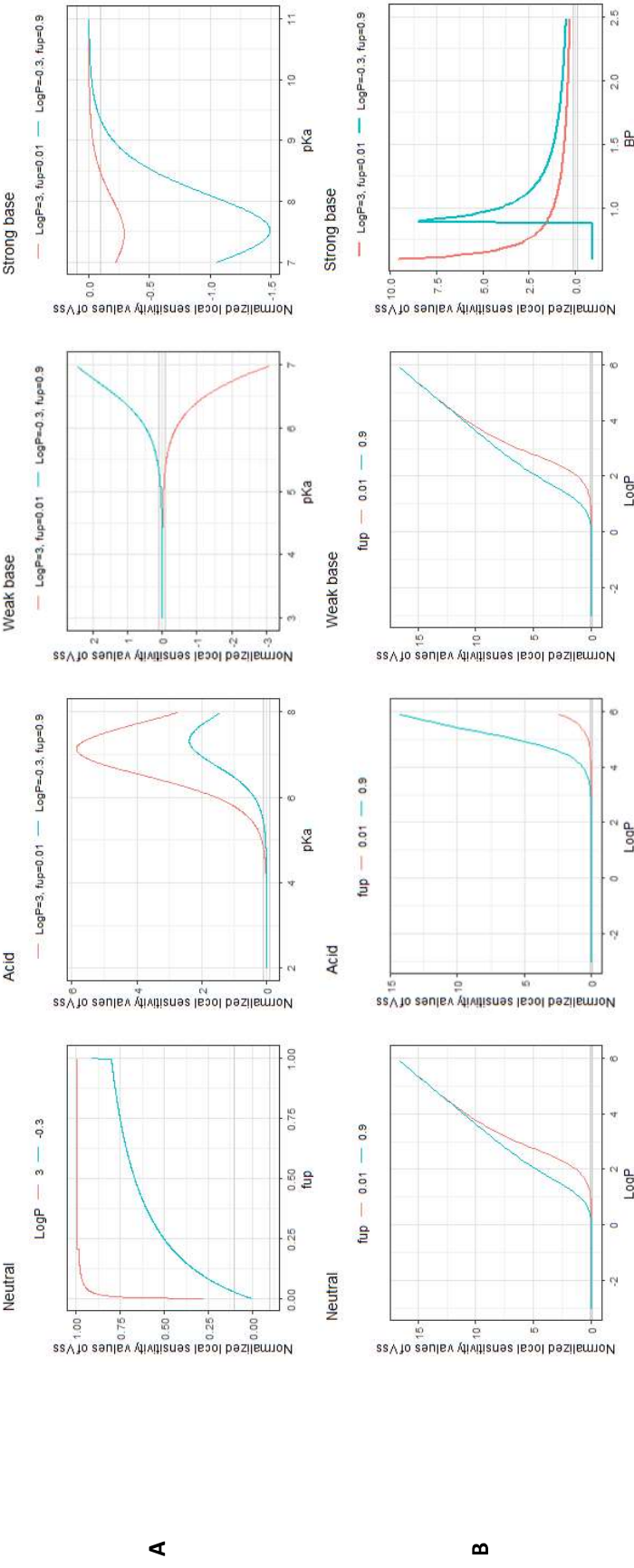
Figure 2: Parameter ranking determined by the PRCC of tissue K_{pu} for weak and strong bases with different relationship between $\log P$ and fraction unbound in plasma (f_{up}) for weak and strong bases

LogP and f_{up} relationship	Weak base			Strong base		
	Parameter ranking determined by the PRCC			Parameter ranking determined by the PRCC		
Independent	f_{up} 2 1 3	$\log P$ 2 1 3	pKa 2 1 3	f_{up} 2 1 3	$\log P$ 2 1 3	pKa 2 1 3
Correlation of $p=0.3$	f_{up} 2 1 3	$\log P$ 2 1 3	pKa 2 1 3	f_{up} 2 1 3	$\log P$ 2 1 3	pKa 2 1 3
Correlation of $p=0.5$	f_{up} 2 1 3	$\log P$ 2 1 3	pKa 2 1 3	f_{up} 2 1 3	$\log P$ 2 1 3	pKa 2 1 3
Correlation of $p=0.9$	f_{up} 2 1 3	$\log P$ 2 1 3	pKa 2 1 3	f_{up} 2 1 3	$\log P$ 2 1 3	pKa 2 1 3
Nonlinear with f_{up} (Yamazaki)	f_{up} 2 1 3	$\log P$ 2 1 3	pKa 2 1 3	f_{up} 2 1 3	$\log P$ 2 1 3	pKa 2 1 3

rob: rest of body; RBC: Red blood cell

Parameter sensitivity ranking from most to less: blue (1), green (2), yellow (3), red (4)

Figure 3: Normalized local SA values (S_i) of V_{ss} with respect to (A) the least influential drug parameter (f_{up} or pK_a) or (B) the most influential drug parameter (LogP or BP)



Red line: Compound with high lipophilicity/low binding; Blue line: Compound with low lipophilicity/high binding
 f_{up} was varied in increments of 0.001 from 0.001 to 1 ; pK_a values were varied in increments of 0.01 ; LogP was varied in increments of 0.01 ; BP was varied in increments of 0.1 ; BP was varied in increments of 0.01 from 0.6 to 2.5 for an acid ($pK_a=3$), a weak base ($pK_a=6$) and a strong base ($pK_a=8$).

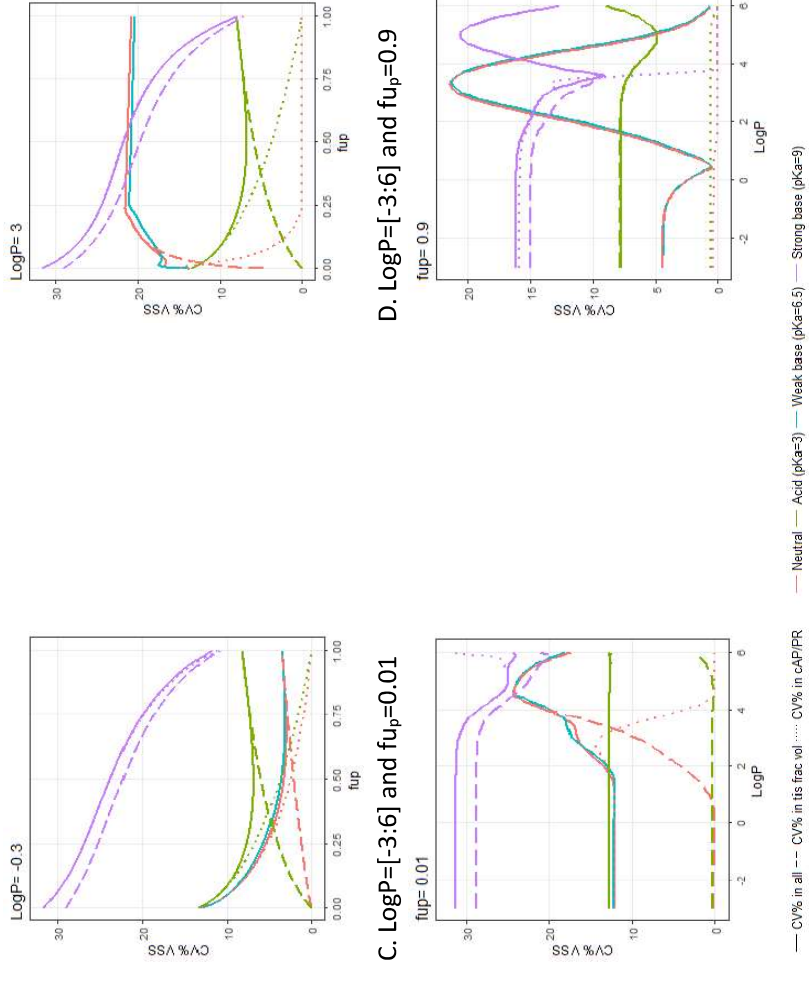
Figure 4: Effect of inputting CV30% simultaneously or individually on fractional tissue volumes and/or all tissue acidic phospholipids/ extracellular protein ratios when varying f_{u_p} or LogP on V_{ss} for a hypothetical neutral (red), acidic (green), weakly basic (blue) and strongly basic (purple) basic compound

A. $\text{LogP}=-0.3$ and $f_{u_p}=0.001:1$

B. $\text{LogP}=3$ and $f_{u_p}=0.001:1$

C. $\text{LogP}=[-3:6]$ and $f_{u_p}=0.01$

D. $\text{LogP}=[-3:6]$ and $f_{u_p}=0.9$



Legend to Figures

Figure 1: Parameter ranking determined by the PRCC of tissue K_{pus} for each drug class with different relationships between LogP and fraction unbound in plasma (f_{u_p}) for neutral and acidic compounds

Rob: rest of body; RBC: Red blood cell

Parameter sensitivity ranking from most to less: blue (1), green (2), yellow (3), red (4)

Figure 2: Parameter ranking determined by the PRCC of tissue K_{pus} for weak and strong bases with different relationship between LogP and fraction unbound in plasma (f_{u_p}) for weak and strong bases

Rob: rest of body; RBC: Red blood cell

Parameter sensitivity ranking from most to less: blue (1), green (2), yellow (3), red (4)

Figure 3: Normalized local SA values (S_{ij}) of V_{ss} with respect to (A) the least influential drug parameter (f_{u_p} or pKa) or (B) the most influential drug parameter (LogP or BP)

Red line: Compound with high lipophilicity/low binding; Blue line: Compound with low lipophilicity/high binding

f_{u_p} was varied in increments of 0.001 from 0.001 to 1; pKa values were varied in increments of 0.01; LogP was varied in increments of 0.1; BP was varied in increments of 0.01 from 0.6 to 2.5 for an acid (pKa=3), a weak base (pKa=6) and a strong base (pKa=8)

Figure 4: Effect of inputting CV30% simultaneously or individually on fractional tissue volumes and/or all tissue acidic phospholipids/ extracellular protein ratios when varying f_{u_p} or LogP on V_{ss} for a hypothetical neutral (red), acidic (green), weakly basic (blue) and strongly basic (purple) basic compound

Solid line: CV30% on fractional tissue volumes and all tissue acidic phospholipids/extracellular protein ratios; Dashed line: CV30% only on fractional tissue volumes; Dotted line: CV30% on all tissue acidic phospholipids/ extracellular protein ratios